PERGAMON

Journal of Structural Geology 23 (2001) 343–353

JOURNAL OF STRUCTURAL GEOLOGY

www.elsevier.nl/locate/jstrugeo

# Fracture networks and fluid transport in active fault zones

Agust Gudmundsson*, Silje S. Berg, Kellfrid B. Lyslo, Elin Skurtveit

*Geological Institute, University of Bergen, Allegt. 41, N-5007 Bergen, Norway*

Received 14 February 1999; accepted 19 June 2000

**Abstract**

Field measurements were made of 1717 mineral-filled veins in the damage zone of an active dextral strike-slip fault zone in Iceland. Most veins are composed of quartz, chalcedony and zeolites, strike roughly parallel or perpendicular to the fault zone, and are members of dense palaeo-fluid transporting networks. A common vein frequency in these networks is 10 veins per metre. Cross-cutting relationships indicate that 79% of the veins are extension (mode I) cracks and 21% are shear cracks. The apertures of most veins, measured as mineral-fill thicknesses, are from 0.1 to 85 mm, and the aperture frequency distribution is a power law. The outcrop trace lengths of 384 veins (of the 1717) could be measured accurately. These 384 veins are mostly small and range in length from 2.5 to 400 cm, in aperture from 0.01 to 0.9 cm, and have an average length/aperture ratio of about 400. Simple analytical models are derived and used to make rough estimates of the volumetric flow rates in hydrofractures of dimensions equal to those of typical veins. The results indicate that volumetric flow rates for a horizontal fracture and a vertical fracture in a rigid (non-deforming) host rock would be around $1.5 \times 10^{-4}$ and $8.9 \times 10^{-4}$ $m^3 s^{-1}$, respectively. The volumetric flow rate in a vertical fracture of equal size but in a deforming host rock, with buoyancy added to the pressure gradient, is around $1.3 \times 10^{-3}$ $m^3 s^{-1}$. Thus, vertical fluid transport is favoured under these conditions. 

## 1. Introduction

There is increasing evidence for a close interaction between fluids and faulting (e.g. Hickman et al., 1995; Ingebritsen and Sanford, 1998; Haneberg et al., 1999; Hardebeck and Hauksson, 1999). Not only are fluids commonly driven to, and flow along, fault zones, but overpressured fluids may trigger fault slip in these zones (e.g. Hickman et al., 1995). This interaction is important in various fields of earth sciences, including structural geology, petroleum geology, seismology and hydrogeology. Because of this importance, detailed studies have been made of the permeability structures of fault zones, using laboratory and theoretical approaches (e.g. Chester and Logan, 1986; Caine et al., 1996; Sibson, 1996; Evans et al., 1997; Seront et al., 1998; Caine and Forster, 1999; Haneberg et al., 1999), as well as direct field measurements (e.g. Ahlbom and Smellie, 1991; Barton et al., 1995; Braathen et al., 1999).

Notwithstanding this work, fluid flow in and towards fault zones is a topic that is still not well understood. For example, during periods prior to mainshocks, there are commonly hydraulic changes in the host rock, such as those regarding spring yields and water-table levels, out to great distances from the faults (Roeloffs, 1988). By contrast, other active faults that produce equally large earthquakes lack concurrent major hydraulic changes. Similarly, fault slips associated with some earthquakes result in large temporary hydraulic changes, whereas other slips, related to earthquakes of equal or greater magnitude, do not lead to noticeable changes (Muirwood and King, 1993; Rojskczer et al., 1995).

The two main hydrogeological structures of major fault zones (Fig. 1) are the core, consisting mainly of breccia and other cataclastic rocks, and the fault damage zone, consisting mainly of fractures of various sizes (e.g. Bruhn et al., 1994; Caine et al., 1996; Evans et al., 1997; Seront et al., 1998). Fluid transport in the damage zone is through fractures that commonly form dense networks (Caine et al., 1996; Sibson, 1996, 2000). In a well-exposed network, accurate measurements can normally be made of the fracture attitudes, but accurate measurements of fracture outcrop lengths and apertures are normally much more difficult. For fracture outcrop length measurements to be useful in analytical models, the fracture must be continuous and both its ends exposed and unrestricted by other discontinuities. Similarly, apertures of small-scale fractures such as are abundant in the damage zones of fault zones are commonly at or below the resolution limit of field measurements and difficult to define accurately. When fractures are

* Corresponding author. Tel.: +47-5558-9416; fax: +47-5558-3521.
*E-mail address:* agust.gudmundsson@geol.uib.no (A. Gudmundsson).

0191-8141/01/$ - see front matter 
PII: S0191-8141(00)00100-0

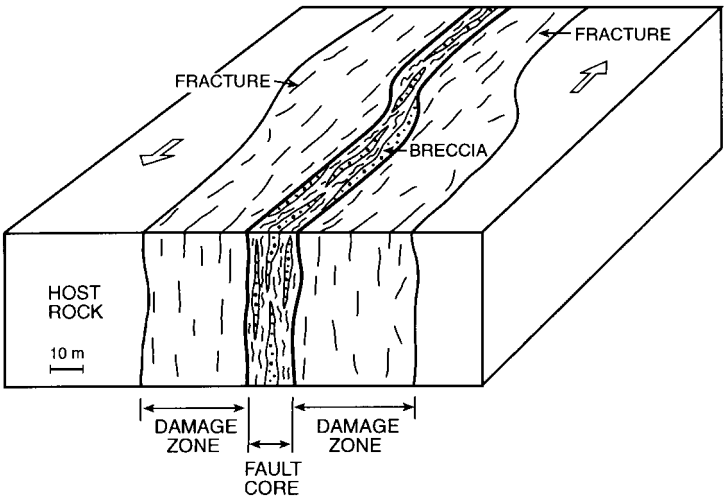


Fig. 1. Schematic infrastructure of a large-scale strike-slip fault zone. Fault slip occurs mostly along the core, which consists primarily of breccia and other cataclastic rocks. The damage zone contains numerous faults and fractures. For a major fault zone, the core thickness is up to several tens of metres and the damage-zone thickness up to several hundred metres (data from Chester and Logan, 1986; Smith et al., 1990; Bruhn et al., 1994; Caine et al., 1996; and the authors' observations).

studied in road cuts or in tunnels, there is the additional problem of aperture increase during the road construction.

Many models of the flow of crustal fluids in rock fractures, particularly those dealing with flow of groundwater in fracture systems in the uppermost part of the crust (e.g. Bear, 1993; Taylor et al., 1999), assume the host rock to be perfectly rigid. This implies that the host rock does not deform during the fluid transport, so that the potential effects of buoyancy on the pressure gradient of the fluid can be neglected. At deeper crustal levels, particularly in active and often weak fault zones, the fluid sources are likely to deform when the fluid is transported, in which case buoyancy should be taken into account.

This paper has two principal aims. First, to provide detailed field data on mineral-filled veins that constitute an important part of the palaeofluid-transporting fracture network in the damage zone of an active strike-slip fault zone in North Iceland (Fig. 2). In particular, the paper presents the results of aperture measurements of 1717 fault-related veins and outcrop-length measurements of 384 veins. Second, to use these data, conceptualised as individual vertical and horizontal hydrofractures, to provide simple, quantitative models of fluid transport during flow in the damage zone of a typical, major active strike-slip fault zone.

## 2. Fracture networks

When fluid-transporting fractures in fault zones gradually become sealed with minerals, their damage zones may develop dense networks of mineral-filled fractures, referred to as veins. To study the geometry of fluid-transporting systems in active fault zones, we measured 1717 mineral-filled veins in the on-land parts of the Husavik-Flatey Fault in North Iceland (Fig. 2). A dextral strike-slip fault with a cumulative displacement of roughly 60 km (Gudmundsson, 1995a; Rognvaldsson et al., 1998), the Husavik-Flatey Fault forms a part of an oceanic transform fault, the Tjornes Fracture Zone. The Husavik-Flatey Fault, initiated at 7-9 Ma, is still one of the most active seismic zones in Iceland (Gudmundsson, 1995b; Rognvaldsson et al., 1998). The studied outcrops are at the coast of the Flateyjarskagi Peninsula, where the crustal depth is estimated at roughly 1500 m below the initial top of the 10- to 12-Ma-old basaltic lava pile that the fault dissects.

The damage-zone veins, primarily composed of quartz, chalcedony and zeolites, form dense networks in the basaltic lava flows (Fig. 3). The average intensity in the studied networks is around 10 veins per metre of the measured profile. The geometrical parameters, such as attitude, aperture, type of displacement, cross-cutting relationships with other veins and amygdales, and the variation in aperture along selected veins, were measured in subvertical and subhorizontal profiles trending roughly perpendicular to the main trends of veins (Fig. 3).

Of 829 studied cross-cutting relationships between the veins (Fig. 4), only 21% show evidence of shear displacement, whereas 79% appear to be extension (mode I) cracks. All the veins with shear displacement are strike-slip faults; in 12% the displacement sense is sinistral, in the remaining 9% it is dextral.

Most veins strike either subparallel, or subperpendicular (Fig. 5), to the main trend, N65°W, of the fault zone (Fig. 2). As is common in transform faults (Gudmundsson, 1995b), the Husavik-Flatey Fault is partly a graben structure, and thus subject to transform-perpendicular extension, in addition to being subject to transform-parallel displacement. The NNE-trending veins (Fig. 5) strike roughly perpendicular to the time-averaged spreading vector, and may thus be largely

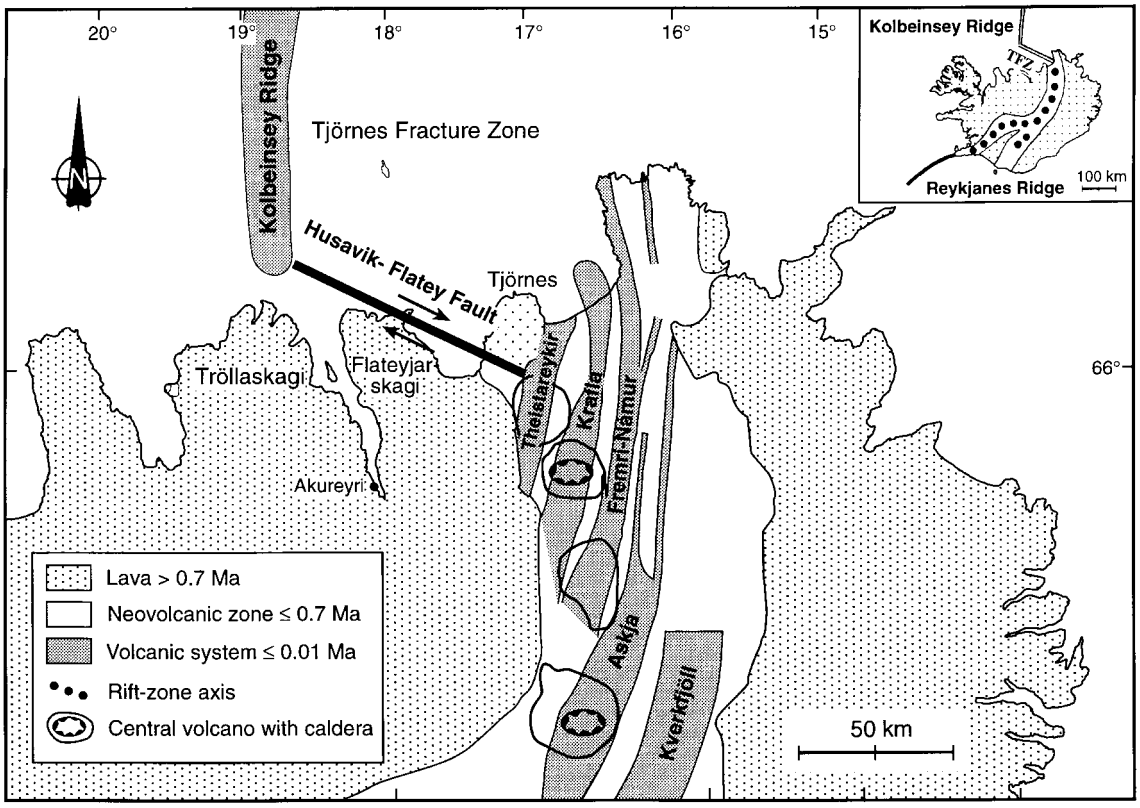


Fig. 2. The Husavik-Flatey Fault, an active dextral strike-slip fault partly exposed on land on the Flateyjarskagi Peninsula, runs parallel with the spreading vector in this part of Iceland and is the main structure of the Tjornes Fracture Zone transform fault (modified from Gudmundsson, 2000).

explained by a spreading-generated minimum horizontal stress that is subparallel with the Husavik-Flatey Fault. By contrast, the W-trending veins may be largely related to the transform-perpendicular extension during graben formation along the fault.

In the measured networks, most veins range in aperture from 0.1 to 85 mm (Fig. 6), but outside the networks the apertures of some veins reach 100 mm. Many veins show evidence of reactivation and repeated injections of fluids, as is common (e.g. Ramsay, 1980; Fisher and Brantley, 1992). The frequency distribution of a vein aperture is interpreted as a power law over the sample-size range (Fig. 6); thus, there are many thin veins but very few thick ones. Most veins belong to networks where they commonly cross-cut. These veins have restricted lengths (Figs. 3 and 4) in the sense that they reach the surface of the body within which

Fig. 3. Veins in the damage zone of the Husavik-Flatey Fault (Fig. 2) form dense networks. The veins were measured in profiles (like the one along the white measuring tape). See the person at the right margin of the photograph for scale.

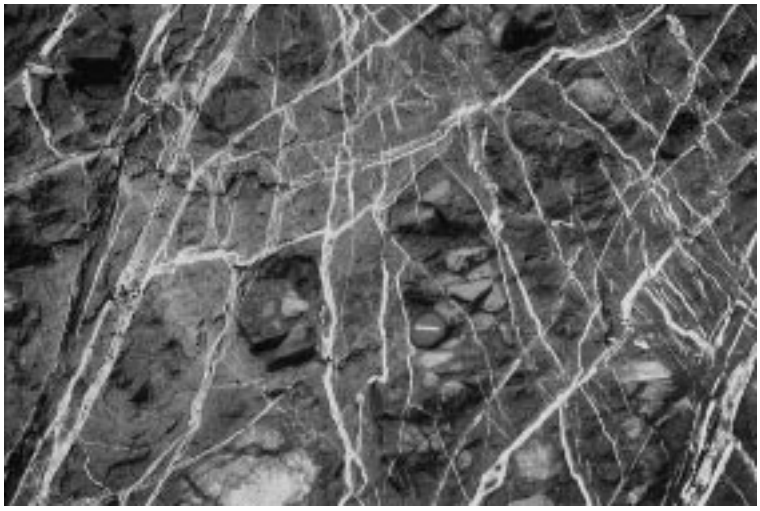

Fig. 4. Close-up view of the central part of the vein network in Fig. 3. Cross-cutting relationships indicate that most veins are extension fractures, whereas some are small-scale strike-slip faults. See the camera lens for scale.

they occur or meet with other fractures or discontinuities (Nicol et al., 1996), and cannot be used for estimating fluid pressure (Gudmundsson, 1983, 1999).

Of the 1717 measured veins, however, 384 unrestricted veins could be used to estimate fluid overpressure, being mode I cracks with both (mostly lateral) ends visible. Defining the vein-outcrop length as the linear distance between its two ends, so that all discontinuous veins are regarded as separate veins, these veins range in length from 2.5 to 400 cm (Fig. 7), and in aperture from 0.01 to 0.9 cm. The average ratio between vein-outcrop length and the maximum aperture is roughly 400 (Fig. 8). These results can be used to estimate the average fluid overpressure during vein emplacement.

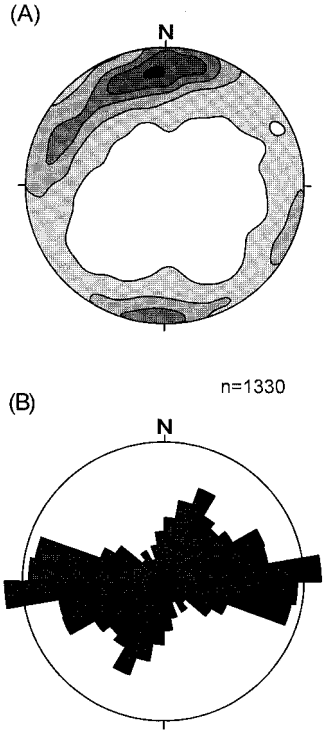


Fig. 5. Stereo plot (A) and rose diagram (B) of 1333 veins in the damage zone of the Husavik-Flatey Fault. (A) The plot is an equal area, lower hemisphere, conventional plot of the projection of poles to the veins. The contours are at intervals of 13.3%. (B) The class limits (widths) are 5° and the circle radius is 3%.

## 3. Fluid flow in fault zones

Fluid flow along a single fracture modelled as flow between parallel, smooth plates is a well-known special solution to the Navier–Stokes equation for the flow of a viscous fluid (e.g. Milne-Thompson, 1996; Nakayama and Boucher, 1999). It is widely used in hydrogeology, where it is commonly referred to as the cubic law (Bear, 1993). Here, we use this solution as a basis for an analytical study of fluid flow in vertical and horizontal fractures in the damage zone of a fault zone.

Consider flow in a fracture, of any attitude, with aperture $b$ and width $W$ in a direction that is perpendicular to the flow direction (Fig. 9). The cross-sectional area of the fracture perpendicular to the flow is thus $A = bW$. The volumetric flow rate $Q$, i.e. the volume of fluid flowing in unit time through the fracture, is then given by:

$$Q = -\frac{b^3 W \rho_w g}{12\mu} \nabla h, \tag{1}$$

where $\rho_w$ is the density of the water (or other fluid), $g$ the acceleration due to gravity, $\mu$ the dynamic (absolute) viscosity of the water and $\nabla h$ the gradient of the hydraulic head $h$, defined by:

$$h = \frac{P}{\rho_w g} + z^*, \tag{2}$$

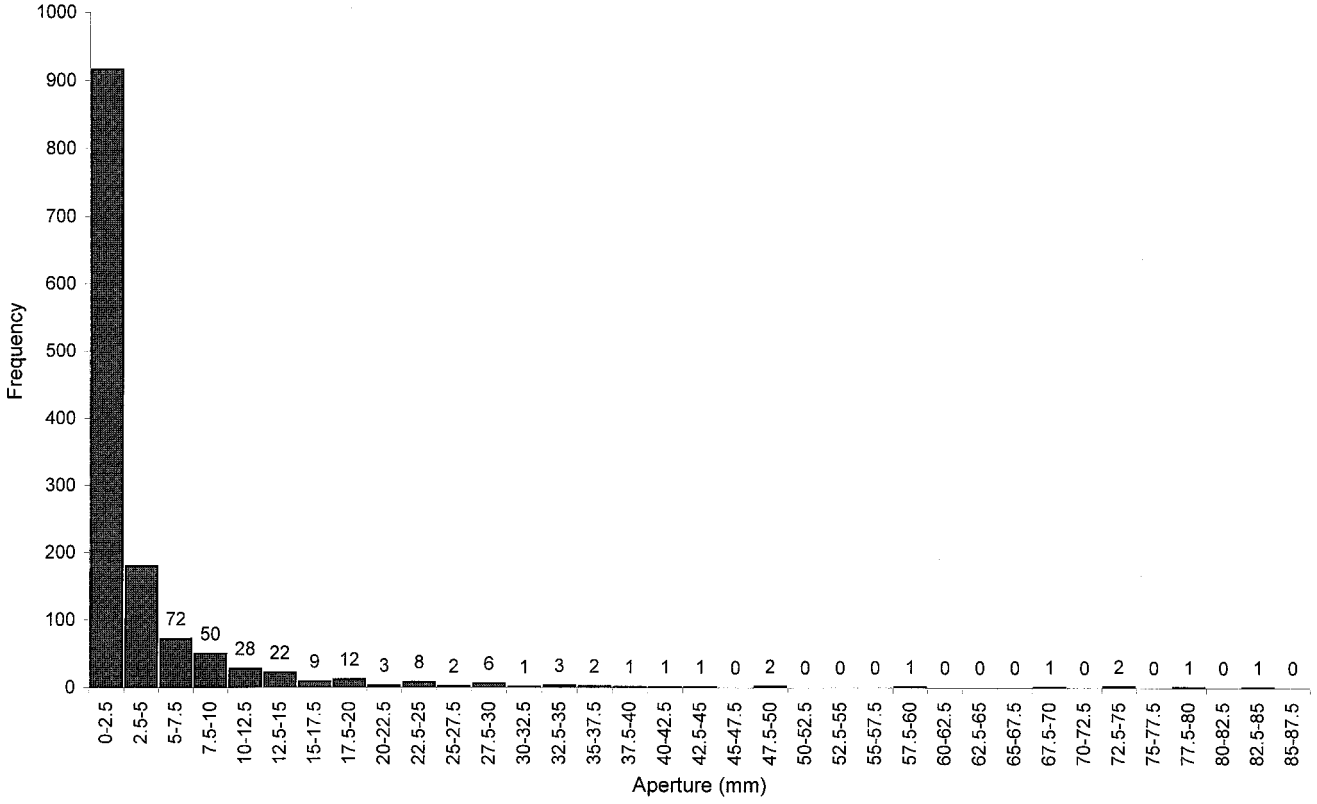


Fig. 6. Aperture frequency distribution (also shown as numbers above most classes) of 1333 veins in the fracture networks of the damage zone of the Husavik-Flatey Fault. These veins range in thickness from 0.1 to 85 mm.

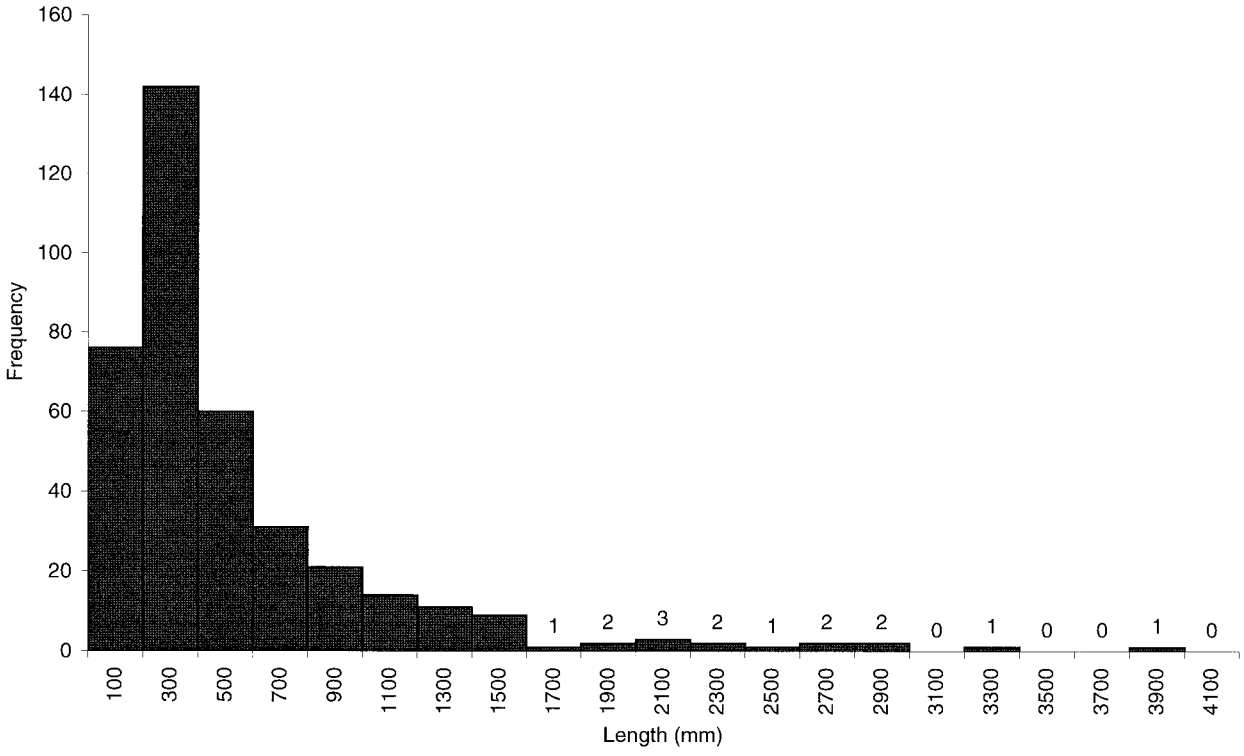


Fig. 7. Outcrop-length frequency distribution of 384 veins in the damage zone of the Husavik-Flatey Fault.

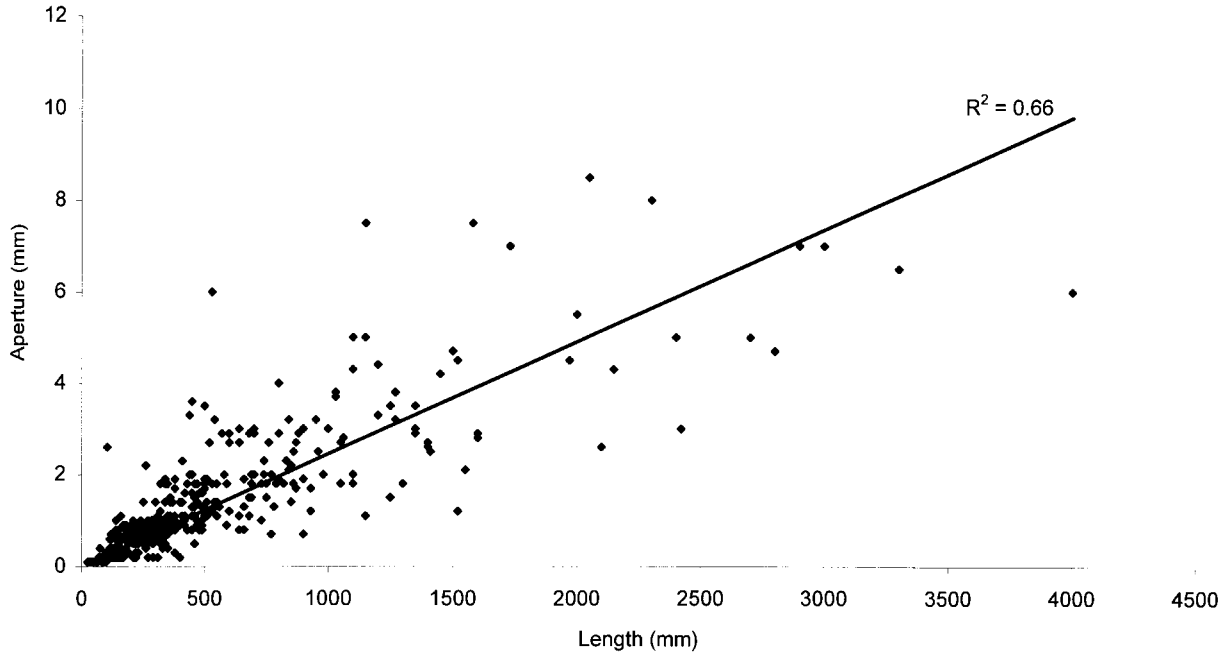


Fig. 8. Outcrop length versus aperture of 384 veins in the damage zone of the Husavik-Flatey Fault. The average aspect ratio (length/aperture) of these veins is around 400. The linear regression line (forced through the origin) has a coefficient of determination of $R^2 = 0.66$ and thus a linear correlation coefficient of $R = 0.81$.

where $P$ is the total fluid pressure at the bottom of a drillhole (piezometer), located at a certain elevation $z^*$ (elevation head) above a reference level (usually sea level in hydrogeology). $Q$ is a function of both location and time. Crustal fluids flow in the direction of decreasing total head, as given by Eq. (2); thus, Eq. (1) includes a minus sign.

### 3.1. Vertical flow

Consider now the flow of fluid in a vertical fracture from a fluid reservoir or a source in a fault zone. Many subhorizontal veins—water sills (Sun, 1969; Fyfe et al., 1978)—may have acted as sources for the subvertical veins (Gudmundsson, 1999, Fig. 2) and vice versa. For convenience, we will here take the source of a vertical hydrofracture as a horizontal fluid-filled fracture, a sill (Fig. 9), but the general modelling results do not depend on that source geometry. If the sill is subject to internal fluid excess pressure, $p_e$ (in excess of the compressive stress on the roof of the sill), the condition for the rupture and initiation of a hydrofracture is:

$$p_l + p_e \geq \sigma_3 + T_0, \tag{3}$$

where $p_l$ is the lithostatic stress at the depth of the sill,

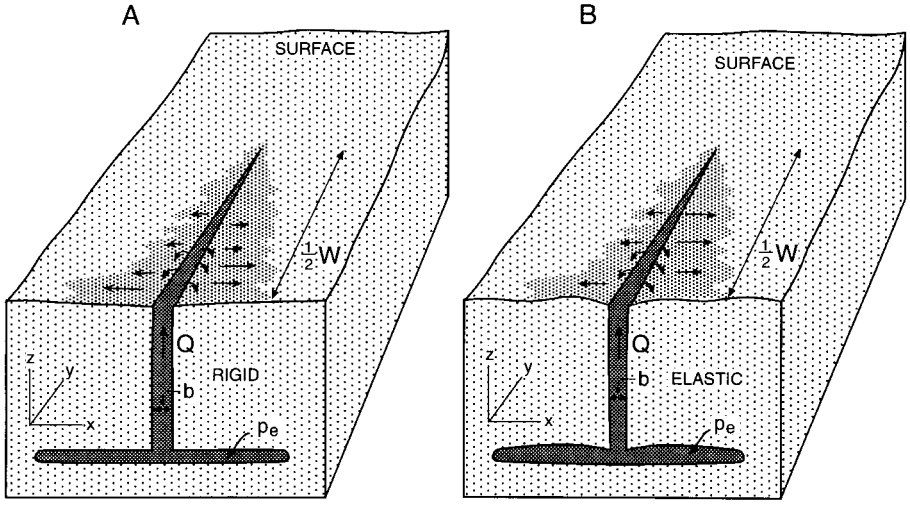


Fig. 9. Schematic models of a vertical hydrofracture being supplied with water from a horizontal water sill. The aperture, $b$, half the width, $W$, volumetric fluid flow, $Q$, and excess fluid pressure, $p_e$, are indicated. (A) In a rigid host rock. (B) In an elastic host rock.

$p_e = P - p_l$ is the excess fluid pressure, which is the difference between the total fluid pressure, $P$, in the sill at the time of its rupture and the lithostatic pressure, $\sigma_3$ is the minimum compressive (considered positive) principal stress, acting perpendicular to the hydrofracture, and $T_0$ is the in situ tensile strength of the host rock in the roof of the sill. Because it is the pressure during rupture of the sill roof which is of concern here, the datum or reference level used in defining the total head in Eq. (2), usually set at sea level, coincides here with the roof of the sill (the rock–fluid contact). Furthermore, the fluid pressure inducing the hydrofracture is measured at this same level, so that the elevation head $z^*$ in Eq. (2) is zero. Differentiating Eq. (2) with respect to the vertical coordinate, $z$, and with $z^* = 0$, we get:

$$\frac{\partial h}{\partial z} = \frac{\partial}{\partial z}\left(\frac{P}{\rho_w g}\right) = \frac{1}{\rho_w g}\frac{\partial P}{\partial z}, \tag{4}$$

where, from Eq. (2) and taking into account the excess pressure in Eq. (3) at the site of hydrofracture initiation, the total fluid pressure $P$ is:

$$P = -\rho_w g z + p_e, \tag{5}$$

where the minus sign is because $z$ is positive upwards.

The rock can respond to the propagation of a vertical hydrofracture in two basic ways. First, the resulting fracture (and its fluid source, the sill) may be entirely self-supporting, non-deforming, in which case the host rock would be rigid (Fig. 9a). Second, the host rock, including the sill, may respond to the water transport by deforming, commonly in an elastic way, as the fluid pressure changes (Fig. 9b).

Consider first the case of vertical fluid flow in a self-supporting fracture, an assumption frequently made in considering groundwater transport in hydrogeology (Bear, 1993). For the volumetric rate $Q$ (Fig. 9a), we use the subscript $z$ to denote the direction of the flow and the superscript $s$ to indicate that the fracture is self-supporting. Then, from Eqs. (1), (4) and (5), we obtain:

$$Q_z^s = \frac{b^3 W}{12\mu}\left(\rho_w g - \frac{\partial p_e}{\partial z}\right). \tag{6}$$

Because the first two terms on the right side of the equation are initially negative, on multiplication they become positive, whereas the third term becomes negative.

Consider next the case where the walls are free to deform as the fluid is transported from the sill and up through the vertical fracture (Fig. 9b). Then, the weight of the rock above the sill must be supported by its internal fluid pressure and, because the density of the host rock, $\rho_r$, is different from that of the fluid, $\rho_w$, a buoyancy term must be added to Eq. (5), which then becomes:

$$P = -(\rho_r - \rho_w) g z + p_e. \tag{7}$$

Using the subscript $z$ to denote the direction of the flow and the superscript $e$ to indicate that the vertical fracture is being supplied with fluid from an elastically deforming source, from Eqs. (1), (4) and (7), the volumetric rate of fluid flow in a vertical fracture is:

$$Q_z^e = \frac{b^3 W}{12\mu}\left[(\rho_r - \rho_w) g - \frac{\partial p_e}{\partial z}\right]. \tag{8}$$

In this equation, the fracture aperture, $b$, is assumed constant, whereas it would normally depend on the fluid pressure in the fracture and the state of stress in the elastic host rock. These effects are discussed in the section on fluid pressure and fracture shape (cf. Valko and Economides, 1995).

### 3.2. Horizontal flow

We again use the model of flow between smooth, parallel plates. Here, we consider only horizontal flow (along the $x$-axis) of a fluid of viscosity $\mu$ in a self-supporting (rigid) fracture of aperture $b$ and width $W$ (measured along the $y$-axis) perpendicular to the flow. In this case, the first term on the right side of Eq. (5) is zero, so that $P = p_e$. Using the subscript $x$ to denote the direction of the flow and the superscript $s$ to denote a self-supporting fracture, from Eq. (1), and by analogy with Eq. (6), we obtain:

$$Q_x^s = -\frac{b^3 W}{12\mu}\frac{\partial p_e}{\partial x}, \tag{9}$$

where the minus sign is because the horizontal fluid flow is in the direction of decreasing pressure.

## 4. Fluid pressure and fracture shape

The shape of a fracture in a rigid host rock does not depend on its fluid pressure, whereas that of a fracture in an elastic (or otherwise deforming) host rock does. For example, for a circular (penny-shaped) interior crack, the displacement or half the aperture, $u$, varies along the radial coordinate, $r$, as (e.g. Sneddon, 1951):

$$u(r) = \frac{4P_o(1-\nu^2)}{\pi E}(a^2 - r^2)^{1/2}, \tag{10}$$

where $a$ is the radius of the hydrofracture, $\nu$ is Poisson's ratio of the host rock, $E$ its Young's modulus and $P_o$ is a measure of how much the fluid pressure exceeds the stress normal to the fracture, which for the mode I cracks under consideration is the minimum principal compressive stress $\sigma_3$. $P_o$ depends on the excess pressure $p_e$ in the source, on the buoyancy effect and the state of stress in the host rock, and is the pressure available to drive the fracture walls open at a particular point. $P_o$ is variously referred to as net pressure (Valko and Economides, 1995), driving pressure (Pollard and Muller, 1976; Pollard and Segall, 1987), driving stress (Pollard and Segall, 1987; Vermilye and Scholz, 1995) and overpressure (Amadei and Stephansson, 1997; Bonafede and Rivalta, 1999; Gudmundsson, 1999; Sibson, 2000). We refer to $P_o$ as overpressure. It is not to

be confused with an abnormal pore pressure in formations (Hubbert and Rubey, 1959; Chapman, 1981; Dahlberg, 1995). Hydrostatic pressure is then regarded as normal, and formation pressures that are less than hydrostatic are commonly referred to as subnormal, whereas those that are greater than hydrostatic are referred to as supernormal (Selley, 1998).

Most veins that we studied in the fault damage zones are mode I cracks. Such hydrofractures propagate in a principal stress plane which includes the maximum compressive stress, $\sigma_1$, and is perpendicular to the minimum compressive stress, $\sigma_3$. From Eq. (10), the maximum aperture of a hydrofracture, $b_{max} = 2u_{max}$, occurs in its centre (at $r = 0$), and is given by:

$$b_{max} = \frac{8P_o(1 - \nu^2)a}{\pi E}. \quad (11)$$

Eqs. (10) and (11) are appropriate for horizontal sill-like hydrofractures located at depths below the free surface that are large in comparison with the maximum dimension (strike or dip dimension) of the fracture itself.

Consider next a two-dimensional crack that goes right through the elastic body which contains it, i.e. a through-the-thickness crack (e.g. Atkins and Mai, 1985). If the strike dimension, $L$, is less than the dip dimension (so that $L$ is here identical to $W$ as defined in Eq. (1)), then the aperture $b_{max}$ is related to the strike dimension of the hydrofracture through the equation (Sneddon, 1951; Sneddon and Lowengrub, 1969):

$$b_{max} = \frac{2P_o(1 - \nu^2)L}{E}. \quad (12)$$

Solving Eq. (12) for the fluid overpressure, we obtain:

$$P_o = \frac{b_{max}E}{2L(1 - \nu^2)}. \quad (13)$$

When the fluid overpressure has been obtained from Eq. (13), and using the aspect ratios of measured veins (Fig. 8) and the appropriate elastic moduli of the host rock, the depth $h_s$ to the source of the fluid that formed the vein (the dip dimension or the height of the vertical hydrofracture) can be obtained roughly as (Gudmundsson, 1999):

$$h_s = \frac{P_0 - (p_e + \sigma_d)}{(\rho_r - \rho_w)g}, \quad (14)$$

where $\sigma_d = \sigma_1 - \sigma_3$ is the difference between the principal stresses in the host rock at the crustal depth of the exposure where the veins are measured.

## 5. Application

We now use the analytical formulae derived in the sections above to obtain numerical results on the volumetric flow rates in vertical and horizontal fractures in a damage zone, as well as to make crude estimates of the fluid overpressure at the time of vein emplacement. The assumptions and limitations of these approaches are presented in the Discussion. The basic aim of these numerical examples is to show how very simple analytical models can be used to obtain crude estimates on several parameters related to transport of fluids in active fault zones.

Some of the parameters used in these calculations can vary considerably. These parameters include the in situ tensile strength, $T_0$, which is used to estimate the fluid excess pressure, $p_e$, and Young's modulus, $E$. Also, the dynamic viscosity of the crustal fluid that is being transported depends on its temperature. For example, if the temperature decreases from around 50°C, used in these examples, to around 4°C, a common temperature of cold water springs in Iceland, the dynamic viscosity increases by a factor of nearly 3.

### 5.1. Fluid transport in vertical and horizontal fractures

Normally, when the excess fluid pressure in the sill reaches the local in situ tensile strength of the rock in its roof, there will be rupture and initiation of a hydrofracture (Fig. 9). The in situ tensile strength of a basaltic lava pile is estimated at 0.5–6 MPa (Haimson and Rummel, 1982; Schultz, 1995), and similar results are obtained for solid rocks of different composition (Amadei and Stephansson, 1997, p. 174). Thus, a typical excess fluid pressure would be close to 3 MPa.

The most common outcrop length of the 384 measured veins is from a few centimetres to 1 m (Fig. 7). We take the typical length as 0.5 m and substitute it for the parameter $W$ in Eqs. (6), (8) and (9). A common aperture (thickness) of these veins is 0.1 cm, or 0.001 m (Fig. 6). The temperature of the water flowing through the networks may have ranged from that typical of cold water springs in Iceland (around 4°C) to that typical of low-temperature geothermal springs (up to or exceeding 100°C). We use an average water temperature of 50°C, for which the dynamic viscosity is about $5.5 \times 10^{-4}$ Pa s and the density 990 kg m$^{-3}$ (Fetter, 1994, p. 631). The acceleration due to gravity is $g = 9.8$ m s$^{-2}$. We use the excess fluid pressure $p_e = T_0 = 3$ MPa and assume that it has the potential to drive the water up 1500 m to the surface of the fault zone to form springs at the time of vein emplacement. It follows that the pressure gradient is $\partial p_e/\partial z = -2000$ Pa m$^{-1}$.

Substituting these values into Eq. (6), we obtain the volumetric flow rate through a vertical fracture in a rigid host rock as $Q_z^s \approx 8.9 \times 10^{-4}$ m$^3$ s$^{-1}$. For the same values, and an average host rock density of 2500 kg m$^{-3}$ (Gudmundsson, 1988), Eq. (8), where buoyancy is taken into account, gives the volumetric flow rate as $Q_z^e \approx 1.3 \times 10^{-3}$ m$^3$ s$^{-1}$. Thus, buoyancy has the effect of increasing the volumetric flow rate through a hydrofracture of a given size in the damage zone of the Husavik-Flatey Fault by a factor of around 1.7. Other things being equal, the buoyancy effect would be greater for crustal fluids

originating at greater depths than 1500 m, because the host rock density increases with depth (Gudmundsson, 1988).

For comparison, consider the flow of water in a horizontal fracture in a rigid rock. Using all the same relevant numerical values as in the calculations for the flow in a vertical rigid-rock fracture, and substituting these into Eq. (9), we obtain the volumetric flow rate as $Q_x^s \approx 1.5 \times 10^{-4}\ \mathrm{m^3\ s^{-1}}$. Thus, for the boundary conditions discussed here, a vertical fracture in a rigid host rock yields nearly six times as much water as a horizontal fracture of equal dimensions in a rigid rock. Furthermore, the yield of both types of fractures in rigid rocks is much exceeded by the yield of a vertical fracture in a host rock that is free to deform and the fluid subject to buoyancy effects.

### 5.2. Fluid pressure and depth of sources

The average outcrop length/maximum aperture ratio of all the 384 veins presented in Fig. 8 is around 400. The veins are inferred to have formed at crustal depths of roughly 1500 m below the initial top of the basaltic lava pile that the Husavik-Flatey Fault dissects. Because the velocity of propagation of a hydrofracture forming a vein is slow in comparison with the velocity of propagation of seismic waves, static rather than dynamic moduli should be used to characterise the elastic response of the host rock to the fluid overpressure. The static Young's modulus and Poisson's ratio of the uppermost 1500 m of the basaltic lava pile in Iceland are estimated at 15 GPa and 0.25, respectively (Gudmundsson, 1988). Using these values and a $b_{\max}/L$ ratio of 1:400, Eq. (13) gives the average fluid overpressure, with reference to the minimum principal compressive stress, during the formation of these veins, as $P_o = 20$ MPa.

Using these results, and Eq. (14), a rough estimate of the depth of the sources of the vertical and horizontal hydrofractures (Fig. 9) can be made. In an active fault zone, the difference between the principal stresses, $\sigma_d$ in Eq. (14), may be limited (by frictional equilibrium on pre-existing, optimally oriented small-scale faults subject to high fluid pressure) to a value of $\sigma_d = 4T_0$ or less (Gudmundsson, 1999; Gudmundsson and Homberg, 1999). If the excess fluid pressure $p_e$ in the sill before rupture is 3 MPa, the average host rock density 2500 kg m$^{-3}$, the water density 990 kg m$^{-3}$ and $g = 9.8\ \mathrm{m\ s^{-2}}$, Eq. (14) gives the average depth of the sills as 338 m.

If the water was hotter than 50°C, its density would be lower; if colder, its density would be higher. A greater uncertainty in this depth estimate, however, is the in situ tensile strength. From Eq. (14) and the condition $\sigma_d = 4T_0$, for the depth $h_s$ to be positive the tensile strength during vein formation cannot have exceeded 4 MPa. A lower tensile strength, however, would increase the estimated depth. For the lowest value quoted above, $p_e = T_0 = 0.5$ MPa, the depth $h_s$ would be 1216 m. Thus, all the results indicate that the studied veins and corresponding hydrofractures originated at shallow depths below the present exposures. While the fluid itself may have been flowing subhorizontally to the fault zone from distances of many tens of kilometres, the water forming the vein networks is likely to have accumulated in sources (sills) at shallow depths below the present exposures in the fault zone.

## 6. Discussion

### 6.1. Assumptions and limitations of the fluid-flow models

Irregularities of the fracture walls, as reflected in relatively great variations in a fracture aperture along its outcrop length, may lead to flow channelling (Tsang and Neretnieks, 1998), whereby the modelling of the fractures by smooth, parallel plates becomes less justifiable. The assumption of a rigid host rock, so that the buoyancy term does not enter into the fluid pressure gradient, may be poor in many active fault zones. This is partly because they normally extend to great depths and elevated temperatures, and partly because they contain fractured and brecciated fault rocks. Many active fault zones are thus likely to be relatively weak and act as a freely deforming host rock to the hydrofractures.

In Eq. (8), we consider only the effects of deformation on the fluid pressure and volumetric flow rate, but not the coupling between fracture aperture, host rock elasticity and fluid pressure. Thus, in the application of this equation to flow in a vertical fracture, a typical aperture, independent of the fluid pressure, is used. Several well-known theoretical models on hydraulically induced fractures consider pressure-related apertures (e.g. Perkins and Kern, 1961; Geertsma and de Klerk, 1969; Sun, 1969; Nordgren, 1972; Abe et al., 1976; Geertsma and Haafkens, 1979). They are all derived from the classic solution for the opening of a Griffith crack under internal fluid pressure (Sneddon, 1951; Sneddon and Lowengrub, 1969). Some of these models have been widely used in analysing hydraulically induced fractures in petroleum engineering, but none of them is regarded as entirely satisfactory in the sense of agreeing with the results of field experiments (Valko and Economides, 1995). There are also many models on dyke propagation, but these are beyond the scope of this paper.

The main limitations of these hydraulic fracture models, from the point of view of problems of fluid flow in active fault zones, are, first, that they are mostly concerned with the lateral propagation of a hydraulically induced fracture in a single layer. Second, with the exceptions of a few models that consider uplift above water sills (e.g. Sun, 1969), nearly all these models assume the hydraulically induced fracture to be vertical and of constant, restricted dip dimension (height). Thus, vertical flow of the fluid is not considered. These assumptions are justified in petroleum engineering because there the main aim is to propagate the fractures laterally, from a fractured well, into the (horizontal) target layer and confine it to that layer. Controlled propagation of

hydraulic fractures in petroleum engineering may thus be very different from that of naturally occurring hydrofractures in an active fault zone, where fractures may propagate in all directions and through many layers with different elastic properties and in situ stresses. The elastic properties and stress fields in different layers have great effects on the shape (Pollard and Muller, 1976) and propagation pathways of the hydrofractures. Many fractures, however, eventually reach the top parts of their fault zone and may transmit large volumes of water to its surface.

### *6.2. Sizes of hydrofractures*

For veins that range in aperture from 0.1 to 100 mm, the outcrop lengths (using 400 as an appropriate aspect ratio) would range from 4 cm to 40 m. These results indicate that the vein lengths are generally much shorter than the distances of fluid transport for which they act as channels. The estimates above indicate that the fluid may have been transported vertically by as much as 1500 m, to the surface of the fault zone. If these size estimates are correct, this transport must occur along veins that are mostly from centimetres to a few metres in outcrop length. Such a result is expected in the case of interconnected networks, as are common in the Husavik-Flatey Fault (Figs. 3 and 4). However, the aspect ratios of the 384 veins are all from unrestricted veins, namely veins that are not visibly parts of networks.

Nevertheless, many of these veins must also be interconnected, through small necks or channels, even if the connections are not visible in the outcrops. Probably, part of the reason for their small sizes is that the veins have very limited fluid volumes available for propagation at any one time. They commonly become arrested when they reach temporary equilibrium lengths, or when they meet with horizontal joints or contacts. On reaching such limits, the hydrofractures must wait for increased volumes of fluid before they can reach the conditions for continuing their propagation.

## 7. Conclusions

The Husavik-Flatey Fault, an active dextral strike-slip fault zone in North Iceland, has a well-exposed damage zone that contains dense networks of veins, composed mostly of quartz, chalcedony and zeolites. Field studies indicate that most of the veins are extension fractures (mode I cracks), formed perpendicular to the minimum compressive principal stress, and are steeply dipping to vertical. The outcrop length/aperture ratio of 384 unrestricted veins is 400. Using this ratio and simple elastic crack models, it is suggested that the fluid pressure in the veins at their time of emplacement exceeded the minimum principal stress by 20 MPa. Modelling fluid flow along single veins as flow between parallel smooth plates, volumetric flow in a vertical hydrofracture exceeds that in a horizontal fracture of the same size by a factor of nearly 6.0 for a rigid host rock. Similarly, the volumetric flow in a vertical hydrofracture in an elastic (deforming) host rock exceeds that in a vertical fracture of the same size in a rigid rock by a factor of around 1.5. The results indicate that in the damage zone of a strike-slip fault zone such as the Husavik-Flatey Fault, a large part of the fluid transport is through dense fracture networks that favour vertical fluid flow.

## Acknowledgements

We wish to pay tribute to the memory of Professor Paul Hancock for his outstanding contributions to Structural Geology. We thank Maria Elina Belardinelli, Maurizio Bonafede, Jonathan Saul Caine, William M. Dunne and Simon Kattenhorn for helpful comments on an earlier version of the manuscript. This work was supported by grants from the European Commission (contracts ENV4-CT97-0536 and EVR1-CT-1999-40002), the Iceland Science Foundation and the Research Council of Norway.

## References

Abe, H., Mura, T., Keer, L.M., 1976. Growth rate of a penny-shaped crack in hydraulic fracturing of rocks. Journal of Geophysical Research 81, 5335–5340.

Ahlbom, K., Smellie, J.A.T., 1991. Overview of the fracture zone project at Finnsjön, Sweden. Journal of Hydrology 126, 1–15.

Amadei, B., Stephansson, O., 1997. Rock Stress and its Measurement. Chapman & Hall, London.

Atkins, A.G., Mai, Y.W., 1985. Elastic and Plastic Fracture. Horwood, Chichester.

Barton, C.A., Zoback, M.D., Moos, D., 1995. Fluid flow along potentially active faults in crystalline rock. Geology 23, 683–686.

Bear, J., 1993. Modeling flow and contaminant transport in fractured rocks. In: Bear, J., Tsang, C.F., de Marsily, G. (Eds.), Flow and Contaminant Transport in Fractured Rock. Academic Press, New York, pp. 1–37.

Bonafede, M., Rivalta, E., 1999. On tensile cracks close to and across the interface between two welded elastic half-spaces. Geophysical Journal International 138, 410–434.

Braathen, A., Berg, S.S., Storro, G., Jaeger, O., Henriksen, H., Gabrielsen, R., 1999. Fracture-zone geometry and groundwater flow; results from fracture studies and drill tests in Sunnfjord. Geological Survey of Norway, Report 99.017, 68 p. (in Norwegian).

Bruhn, R.L., Parry, W.T., Yonkee, W.A., Thompson, T., 1994. Fracturing and hydrothermal alteration in normal fault zones. Pure and Applied Geophysics 142, 609–644.

Caine, J.S., Evans, J.P., Forster, C.B., 1996. Fault zone architecture and permeability structure. Geology 24, 1025–1028.

Caine, J.S., Forster, C.B., 1999. Fault zone architecture and fluid flow: insights from field data and numerical modeling. In: Haneberg, W.C., Mozley, P.S., Moore, J.C., Goodwin, L.B. (Eds.), Faults and Subsurface Fluid Flow in the Shallow Crust. American Geophysical Union, Washington, DC, pp. 101–127.

Chapman, R.E., 1981. Geology and Water. Nijhoff, London.

Chester, F.M., Logan, J.M., 1986. Implications for mechanical properties of brittle faults from observations of the Punchbowl fault zone, California. Pure and Applied Geophysics 124, 79–106.

Dahlberg, E.C., 1995. Applied Hydrodynamics in Petroleum Exploration. 2nd ed. Springer, New York.

Evans, J.P., Forster, C.B., Goddard, J.V., 1997. Permeability of fault-related rocks, and implications for hydraulic structure of fault zones. Journal of Structural Geolology 19, 1393–1404.

Fetter, C.W., 1994. Applied Hydrogeology. Prentice Hall, Englewood Cliffs, NJ.

Fisher, D.M., Brantley, S.L., 1992. Models of quartz overgrowth and vein formation: deformation and episodic fluid flow in an ancient subduction zone. Journal of Geophysical Research 97, 20,043–20,061.

Fyfe, W.S., Price, N.J., Thompson, A.B., 1978. Fluids in the Earth's Crust. Elsevier, New York.

Geertsma, J., de Klerk, F., 1969. A rapid method of predicting width and extent of hydraulically induced fractures. Journal of Petroleum Technology 21, 1571–1581.

Geertsma, J., Haafkens, R., 1979. A comparison of the theories for predicting width and extent of hydraulically induced fractures. Journal of Energy Resources Technology 101, 8–19.

Gudmundsson, A., 1983. Stress estimates from the length/width ratios of fractures. Journal of Structural Geology 5, 623–626.

Gudmundsson, A., 1988. Effect of tensile stress concentration around magma chambers on intrusion and extrusion frequencies. Journal of Volcanology and Geothermal Research 35, 179–194.

Gudmundsson, A., 1995a. Ocean-ridge discontinuities in Iceland. Journal of the Geological Society of London 152, 1011–1015.

Gudmundsson, A., 1995b. Stress fields associated with oceanic transform faults. Earth and Planetary Science Letters 136, 603–614.

Gudmundsson, A., 1999. Fluid overpressure and stress drop in fault zones. Geophysical Research Letters 26, 115–118.

Gudmundsson, A., 2000. Dynamics of volcanic systems in Iceland: example of tectonism and volcanism at juxtaposed hot spot and mid-ocean ridge systems. Annual Review of Earth and Planetary Sciences 28, 107–140.

Gudmundsson, A., Homberg, C., 1999. Evolution of stress fields and faulting in seismic zones. Pure and Applied Geophysics 154, 257–280.

Haimson, B.C., Rummel, F., 1982. Hydrofracturing stress measurements in the Iceland research drilling project drill hole at Reydarfjordur, Iceland. Journal of Geophysical Research 87, 6631–6649.

Haneberg, W.C., Mozley, P.S., Moore, J.C., Goodwin, L.B. (Eds.), 1999. Faults and Subsurface Fluid Flow in the Shallow Crust. American Geophysical Union, Washington, DC.

Hardebeck, J.L., Hauksson, E., 1999. Role of fluids in faulting inferred from stress field signatures. Science 285, 236–239.

Hickman, S., Sibson, R.H., Bruhn, R., 1995. Introduction to special section: mechanical involvement of fluids in faulting. Journal of Geophysical Research 100, 12,831–12,840.

Hubbert, M.K., Rubey, W.W., 1959. Role of fluid pressure in the mechanics of overthrust faulting. Bulletin of the Geological Society of America 70, 115–166.

Ingebritsen, S.E., Sanford, W.E., 1998. Groundwater in Geologic Processes. Cambridge University Press, Cambridge.

Milne-Thompson, L.M., 1996. Theoretical Hydrodynamics. 5th ed. Dover, New York.

Muirwood, R., King, G.C.P., 1993. Hydrologic signatures of earthquake strain. Journal of Geophysical Research 98, 22035–22068.

Nakayama, Y., Boucher, R.F., 1999. Introduction to Fluid Mechanics. Arnold, London.

Nicol, A., Watterson, J., Walsh, J.J., Childs, C., 1996. The shapes, major axis orientations and displacement pattern of fault surfaces. Journal of Structural Geology 18, 235–248.

Nordgren, R.P., 1972. Propagation of a vertical hydraulic fracture. Society of Petroleum Engineers Journal 12, 306–314.

Perkins, T.K., Kern, L.R., 1961. Width of hydraulic fractures. Journal of Petroleum Technology 13, 937–949.

Pollard, D.D., Muller, O.H., 1976. The effect of gradients in regional stress and magma pressure on the form of sheet intrusions in cross section. Journal of Geophysical Research 81, 975–984.

Pollard, D.D., Segall, P., 1987. Theoretical displacements and stresses near fractures in rock: with applications to faults, joints, veins, dikes and solution surfaces. In: Atkinson, B. (Ed.), Fracture Mechanics of Rock. Academic Press, London, pp. 277–349.

Ramsay, J.G., 1980. The crack-seal mechanism of rock deformation. Nature 284, 135–139.

Roeloffs, E.A., 1988. Hydrologic precursors to earthquakes: a review. Pure and Applied Geophysics 126, 177–209.

Rognvaldsson, S.Th., Gudmundsson, A., Slunga, R., 1998. Seismotectonic analysis of the Tjornes Fracture Zone, an active transform fault in North Iceland. Journal of Geophysical Research 103, 30,117–30,129.

Rojskczer, S., Wolf, S., Michel, R., 1995. Permeability enhancement in the shallow crust as a cause of earthquake-induced hydrological changes. Nature 373, 237–239.

Schultz, R.A., 1995. Limits on strength and deformation properties of jointed basaltic rock masses. Rock Mechanics and Rock Engineering 28, 1–15.

Selley, R.C., 1998. Elements of Petroleum Geology. 2nd ed. Academic Press, London.

Seront, B., Wong, T.F., Caine, J.S., Forster, C.B., Bruhn, R.L., 1998. Laboratory characterisation of hydromechanical properties of a seismogenic normal fault system. Journal of Structural Geology 20, 865–881.

Sibson, R.H., 1996. Structural permeability of fluid-driven fault-fracture meshes. Journal of Structural Geology 18, 1031–1042.

Sibson, R.H., 2000. Fluid involvement in normal faulting. Journal of Geodynamics 29, 469–499.

Smith, L., Forster, C.B., Evans, J.P., 1990. Interaction between fault zones, fluid flow, and heat transfer at the basin scale. In: Newman, S., Neretnieks, I. (Eds.), Hydrogeology of Low-Permeability Environments, 2. International Association of Hydrogeologists, pp. 41–67.

Sneddon, I.N., 1951. Fourier Transforms. McGraw-Hill, New York.

Sneddon, I.N., Lowengrub, M., 1969. Crack Problems in the Classical Theory of Elasticity. Wiley, New York.

Sun, R.J., 1969. Theoretical size of hydraulically induced horizontal fractures and corresponding surface uplift in an idealized medium. Journal of Geophysical Research 74, 5995–6011.

Taylor, W.L., Pollard, D.D., Aydin, A., 1999. Fluid flow in discrete joint sets: field observations and numerical simulations. Journal of Geophysical Research 104, 28,983–29,006.

Tsang, C.F., Neretnieks, I., 1998. Flow channeling in heterogeneous fractured rocks. Reviews of Geophysics 36, 275–298.

Valko, P., Economides, M.J., 1995. Hydraulic Fracture Mechanics. New York, Wiley.

Vermilye, J.M., Scholz, C.H., 1995. Relation between vein length and aperture. Journal of Structural Geology 17, 423–434.